IEEE Access
Multidisciplinary | Rapid Review | Open Access Journal

Received December 11, 2018, accepted December 21, 2018, date of publication December 27, 2018,
date of current version January 16, 2019.

Digital Object Identifier 10.1109/ACCESS.2018.2889858

Finite-Time Formation Control for Unmanned Aerial Vehicle Swarm System With Time-Delay and Input Saturation

AN ZHANG, DING ZHOU, MI YANG, AND PAN YANG
School of Aeronautics, Northwestern Polytechnical University, Xi'an 710072, China

Corresponding author: Ding Zhou (zhouding@mail.nwpu.edu.cn)

This work was supported in part by the National Natural Science Foundation of China under Grant 61573283.

ABSTRACT This paper deals with finite-time formation control problems of unmanned aerial vehicle swarm system with time-delay and input saturation. Using precise feedback linearization, first, the nonlinear time-delay model of unmanned aerial vehicle is transformed into a linear second-order time-delay system. Based on the neighbors' states, a fixed-time distributed observer is constructed to estimate the leader's state for each follower unmanned aerial vehicle quickly and accurately. Moreover, by utilizing Artstein's transformation, the delayed second-order system is transformed into a delay-free system and a saturation function is used to tackle the input saturation problem. Then, a finite-time formation control protocol is designed based on the Artstein's transformation and saturation function. Rigorous proof shows that all control inputs are bounded and the formation control with time-delay is achieved in finite time. Finally, a simulation example is given to verify the effectiveness of the proposed protocol.

INDEX TERMS Finite-time, formation control, unmanned aerial vehicle swarm, time-delay, input saturation.

I. INTRODUCTION

In the past years, the cooperative formation control of unmanned aerial vehicle (UAV) swarm has attracted an increasing interest due to its broad applications in search and rescue of disaster victims, detection of forest fires, surveillance and reconnaissance [1], [2]. UAV swarm can constitute a much more effective system, which means that some more difficult tasks can be achieved through the cooperation among UAVs. The formation control is a critical step of attempting to control a swarm of UAVs, which control engineers have conducted extensive research for years [3]–[5]. In general, there are two control structures for formation control: centralized structure and distributed structure [4], [6]. Compared with the centralized structure, the distributed control structure has higher reliability and flexibility. Therefore, in this paper, formation control is to develop a distributed control protocol such that all UAVs reach and maintain a desired formation via local interactions.

For different kinds of UAVs, there are three main formation control approaches, which have been developed to investigate the formation control problem, i.e. behavior-based approach [7], leader-follower [8], [9] and virtual structure [10]. Among these formation strategies, the leader-follower approach is widely adopted and has been studied extensively due to its simplicity and scalability. In this architecture, many control protocols have been proposed in the literature for various applications [1], [11], [12]. To solve the problem of multiple UAVs with uncertain parameters, Xu and Zhen proposed a leader-follower control law using multivariable model reference adaptive method, which depended on less information interactions [11]. Furthermore, the close formation problems for this kind of UAV were investigated in the works of Duan and Qiu [12]. For UAV swarm with multiple leaders, the work of He, Bai and Liang investigated the formation control problem without collision among vehicles [1]. For formation control, convergence rate and the ability of disturbance rejection are important performance indexes in practice which have attracted many researchers to study finite-time formation control technique [8], [13]–[15]. For multiple UAVs, Zhao, Chao and Wang proposed a finite-time cooperative formation control protocol based on finite-time control theory and precise feedback linearization [8]. Then, Hu *et al.* [13] investigated finite-time formation control for UAVs with input

quantization and nonholonomic kinematic model based on the backstepping technique. In the work of [14] and [15], the finite-time formation control protocol was proposed for unmanned helicopters.

Note that most of the existing literatures assumed that the actuator of each UAV can generate arbitrary level of control signals and time-delay is avoidable whenever each UAV receives the states of the neighboring UAVs and processes after receipt. Due to the physical structure, aerodynamic configuration, performance of engines and steering gear, input saturation limitation always exists, exceeding which the stability of UAV might be threatened. Especially during the flight, the UAV load burden, wind speed and other factors will affect input saturation of UAV. Recently, these problems mentioned above have been discussed separately for distributed control of robots, spacecrafts and marine vehicles. In the case of input saturation, finite-time formation control approaches were proposed for marine vehicles [16], [17], spacecrafts [18], [20], [21] and robots [22], [23]. For time-delay caused by information transfers and processing, finite-time formation control problems were investigated for spacecrafts [23], [24], robots [25]. In the work of [23] and [24], control protocols were designed by fast terminal sliding manifold and switch function. In the control protocol, only time-delay was considered in the sliding mode, which may make the control protocol not applicable in practical application. Based on [26], [25] proposed a finite-time formation control protocol for non-holonomic robots with communication delay, in which the control parameters need to be very large to ensure the stability. In the practical situation, this approach may exceed the limitation of the actuator and threaten the stability of the closed-loop system. To the best of our knowledge, there is no research on finite-time formation control of UAVs with time-delay and input saturation.

Motivated by the aforementioned discussions, we consider the finite-time formation control problem for UAV swarm with time-delay and input saturation. The main contributions of this paper can be summarized as follows.

(1) Since only the UAV directly connected to the leader UAV can receive the leader's states, a fixed-time observer is constructed for each follower UAV.

(2) To solve the finite-time formation control problem with time-delay, Artstein's transformation is introduced to transform the delayed system into a delay-free system.

(3) A finite-time formation control protocol for UAV swarm is designed based on Artstein's transformation and saturation function. Rigorous proof is given by utilizing homogeneous method and Lyapunov theory.

The remainder of this paper is organized as follows. We first address, in Section 2, preliminaries and problem formulation. In Section 3, precise feedback linearization is first introduced to transform the nonlinear model of UAV into a linear system, then, a finite-time formation control protocol is proposed based on a finite-time observer and Artstein's transformation. Section 4 gives the simulation example. The conclusions and future works are provided in Section 5.

II. PRELIMINARIES AND PROBLEM FORMULATION

A. NOTATIONS AND GRAPH THEORY

Define $sig(p)^{\gamma} = \left[sig(p_1)^{\gamma}, \cdots, sig(p_n)^{\gamma}\right]^T$, $sig(p_i)^{\gamma} = |p_i|^{\gamma} sgn(p_i)$, where $sgn(\bullet)$ is the signum function. I_n and 1_n denote the identity matrix and identity column vector, respectively. $\| \bullet \|$ denotes the 2-norm. $\otimes$ denotes the Kronecker product. R^n denotes n-dimensional Euclidean space.

The topology of n agents is modeled as an undirected graph $G = \{V, \zeta, A\}$, where $\zeta \subseteq \{(i,j), i,j \in V\}$ is the edge set, $V = \{1, 2, \cdots, n\}$ is a finite set of nodes, and $A = \left[a_{ij}\right]_{n\times n}$ is the associated adjacency matrix, where $a_{ii} = 0$, and $a_{ij} = 1$ is the weight if $(j,i) \in \zeta$ or $a_{ij} = 0$, otherwise. The neighbor set of i is defined as $N_i = \left\{j \in V : a_{ij} = 1\right\}$. Denote the matrix $D = diag\{d_{11}, d_{22}, \cdots, d_{nn}\}$ with $d_{ii} = \sum_{j=1, j\neq i}^{n} a_{ij}$. Then, the Laplacian matrix L can be expressed by $L = D - A$ and L is symmetric.

B. DEFINITION AND LEMMAS

Definition 1 [27]: Consider the following system

$$\dot{x} = f(x), \quad f(0) = 0,\ x(0) = x_0,\ x \in R^n$$

where $f(x) : U_0 \mapsto R^n$, $f(x) = (f_1(x), f_2(x), \cdots, f_n(x))$ is continuous on an open neighborhood U_0 of the origin. Let $(r_1, r_2, \cdots, r_n) \in R^n$ with $r_i > 0$. $f(x)$ is homogenous of degree $k \in R$ with respect to $(r_1, r_2, \cdots, r_n)$ if for any given $\varepsilon > 0$, $f_i(\varepsilon^{r_1}x_1, \varepsilon^{r_2}x_2, \cdots, \varepsilon^{r_n}x_n) = \varepsilon^{k+r_i} f_i(x)$, $i = 1, 2, \cdots, n$, $\forall x \in R^n$. $\dot{x} = f(x)$ is said to be homogenous if $f(x)$ is homogenous.

Lemma 1 [27]: Consider the following system

$$\dot{x} = f(x) + \hat{f}(x), \quad f(0) = 0,\ x \in R^n,$$

where $f(x)$ is a continuous homogeneous vector field of degree $k < 0$ with respect to $(r_1, r_2, \cdots, r_n)$ and $\hat{f}(x)$ is a vector function which satisfies $\hat{f}(0) = 0$. Assume that $x = 0$ is an asymptotically stable equilibrium of the system $\dot{x} = f(x)$. Then, $x = 0$ is a locally finite-time stable equilibrium of the system if

$$\lim_{\varepsilon\to 0} \frac{\hat{f}_i(\varepsilon^{r_1}x_1, \cdots, \varepsilon^{r_n}x_n)}{\varepsilon^{k+r_1}} = 0, \quad i = 1, 2, \cdots, n,\ \forall x \neq 0.$$

In addition, the system $\dot{x} = f(x) + \hat{f}(x)$ is globally finite-time stable if the system is globally asymptotically stable and locally finite-time stable.

Lemma 2 [28]: Consider the following system

$$\dot{V} = -\alpha V^{\frac{m}{n}} - \beta V^{\frac{c}{d}}, \quad V(0) = V_0,$$

where m, n, c, d are positive odd integers satisfying $m > n$, $c < d$, $\alpha > 0$ and $\beta > 0$. Then, the equilibrium of the system is globally finite-time stable and the settling time is bounded by

$$T \leq \frac{1}{\alpha}\frac{n}{m-n} + \frac{1}{\beta}\frac{d}{c+d}.$$

Lemma 3 [29]: If $\alpha \in (0, 1]$, *the following inequality holds*

$$\left(\sum_{i=1}^{n}|r_i|\right)^{\alpha} \leq \sum_{i=1}^{n}|r_i|^{\alpha} \leq n^{1-\alpha}\left(\sum_{i=1}^{n}|r_i|\right)^{\alpha},$$

where $r_i \in R$.

Lemma 4 [30]: Consider UAV swarm system, graph for the follower UAVs is connected, and there is at least one UAV that can directly obtain the leader's information. Define diagonal matrix $H = diag\,(a_{10}, a_{20}, \cdots, a_{N0}) \geq 0$ *with* $a_{i0} > 0$ *if the leader is the neighbor of the ith UAV, then* $L+H$ *is positive definite and symmetric.*

Lemma 5 [31]: Consider the system

$$\dot{x}\,(t) = Ax\,(t) + \sum_{i=0}^{k} B_i u\,(t-\tau_i), \quad t \geq 0,$$

where $x\,(t) \in R^n$, $u\,(t) \in R^m$, $A \in R^{n\times n}$, $B_i \in R^{n\times m}$, τ_i *is a positive constant.Let*

$$y\,(t) = x\,(t) + \sum_{i=0}^{k} L^{h_i}_{(A,B_i)} u_t,$$

where $u_t : [-\tau_i, 0] \rightarrow R^m$ *and* $L^{h_i}_{(A,B_i)}u_t = \int_{-\tau_i}^{0} e^{A(-h_i-s)}B_i u\,(t+s)ds$. *Then we have* $\dot{y}\,(t) = Ay\,(t) + Bu\,(t)$ *with* $B = \sum_{i=0}^{k} e^{-Ah_i}B_i$. *If the system* $\dot{y}\,(t) = Ay\,(t) + Bu\,(t)$ *is finite-time stabilizable by a feedback control* $u\,(t) = k\,(t)f\,(y\,(t))$ *with* $k\,(t)$ *bounded and* $f : R^n \rightarrow R^m$ *continuous such that* $f\,(0) = 0$ *and there exists* α *of class K such that* $\|f\,(y)\|_m \leq \alpha\left(\|y\|_n\right)$, *then the system* $y\,(t) = x\,(t) + \sum_{i=0}^{k} L^{h_i}_{(A,B_i)}u_t$ *is finite-time stabilizable by the feedback control* $u\,(t) = k\,(t)f\left(x\,(t) + \sum_{i=0}^{k} L^{h_i}_{(A,B_i)}u_t\right)$.

C. FORMATION CONTROL PROBLEM FORMULATION

Considering UAV swarm system composed of N UAVs (called followers) and a leader UAV (labeled as 0), the graph for all follower UAVs is connected and at least one UAV is connected to the leader. In the practical situation, there is time-delay for each UAV to receive the status of the neighboring UAVs and process after receipt [32], [33]. On the formation control level, the model of the ith UAV is approximately described as follows [8], [34].

$$\begin{cases} \dot{x}_i = V_i \cos\theta_i \cos\psi_i \\ \dot{y}_i = V_i \sin\theta_i \\ \dot{z}_i = -V_i \cos\theta_i \sin\psi_i \\ \dot{V}_i = g\,(\eta_{xi}\,(t-\tau_i) - \sin\theta_i) \\ \dot{\theta}_i = \dfrac{g}{V_i}\left(\eta_{yi}\,(t-\tau_i) - \cos\theta_i\right) \\ \dot{\psi}_i = -\dfrac{g}{V_i\cos\theta_i}\eta_{zi}\,(t-\tau_i), \end{cases} \tag{1}$$

where x_i, y_i, z_i denote the position in the earth-fixed inertial coordinate, V_i is the speed, θ_i is the flight-path angle, ψ_i is the heading angle, g is the acceleration of gravity, $\eta_i = \left[\eta_{xi}, \eta_{yi}, \eta_{zi}\right]^T$ is the control input vector, $\eta_{xi}, \eta_{yi}, \eta_{zi}$ represent the component of overload in the axis of flight path axis coordinates, τ_i denotes the constant input delay of the ith UAV, $i = 1, 2, \cdots, N$.

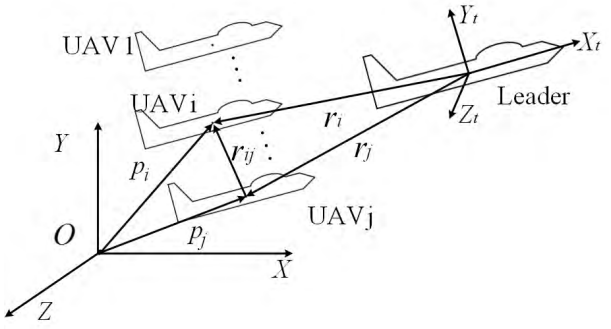

FIGURE 1. The earth-fixed inertial coordinate and flight path axis coordinate.

Without loss of generality, the leader's trajectory is generated by

$$\begin{cases} \dot{x}_0 = V_0 \cos\theta_0 \cos\psi_0 \\ \dot{y}_0 = V_0 \sin\theta_0 \\ \dot{z}_0 = -V_0 \cos\theta_0 \sin\psi_0 \\ \dot{V}_0 = g\,(\eta_{x0}\,(t) - \sin\theta_0) \\ \dot{\theta}_0 = \dfrac{g}{V_0}\left(\eta_{y0}\,(t) - \cos\theta_0\right) \\ \dot{\psi}_0 = -\dfrac{g}{V_0\cos\theta_0}\eta_{z0}\,(t), \end{cases} \tag{2}$$

where x_0, y_0, z_0 denote the leader's position in the earth-fixed inertial coordinate, V_0 is the leader's speed, θ_0 is the leader's flight-path angle, ψ_0 is the leader's heading angle, $\eta_0 = \left[\eta_{x0}, \eta_{y0}, \eta_{z0}\right]^T$ is the leader's control input vector. Let $p_i = [x_i, y_i, z_i]^T$, the earth-fixed inertial coordinate $(O-XYZ)$ and flight path axis coordinate $(O_t - X_tY_tZ_t)$ are depicted by Figure 1.

For UAV swarm system, formation is usually controlled by using distributed control protocol, which is designed on the basis of the neighbors' states. When the number of neighbours increases, it will cause the control input to exceed the limitation of the actuator [35]. The saturation constraint may deteriorate the stability of the controller and even threaten the flight safety of the UAV. It is worth noting that $\eta_i = \left[\eta_{xi}, \eta_{yi}, \eta_{zi}\right]^T$ is the control input in flight path axis coordinates. The limitation of the actuator is the overload limit of earth-fixed inertial coordinate during formation flight, that is, $\|u_i\,(t)\| = \sqrt{u_{ix}^2 + u_{iy}^2 + u_{iz}^2} \leq \|u_{\max}\|$, where $\|u_{\max}\|$ denotes the overload limit, $u_i\,(t) = \left(u_{ix}, u_{iy}, u_{iz}\right)^T$, u_{ix}, u_{iy}, u_{iz} denote the ith UAV's acceleration in earth-fixed inertial coordinate. The goal of finite-time formation control is to design a distributed controller $\|u_i\,(t)\| = \sqrt{u_{ix}^2 + u_{iy}^2 + u_{iz}^2} \leq \|u_{\max}\|$, which can control UAV swarm to

maintain desired formation and track the leader UAV within finite time.

As shown in Figure 1, r_i is the expected position vector between the ith UAV and leader UAV, and r_{ij} is the relative position vector between the ith UAV and jth UAV. Then, the control objective of this paper is to design a distributed controller $\|u_i(t)\| \leq \|u_{\max}\|$ for follower UAVs to satisfy $\lim_{t\to T}\|p_i(t) - r_i - p_0(t)\| = 0$, $\lim_{t\to T}\|\dot{p}_i(t) - \dot{p}_0(t)\| = 0$ and $\|p_i(t) - r_i - p_0(t)\| = 0$, $\|\dot{p}_i(t) - \dot{p}_0(t)\| = 0$ when $t \geq T$, where T denotes a finite-time, $i = 1, 2, \cdots, N$.

III. FINITE-TIME FORMATION CONTROL PROTOCOL DESIGN FOR UAV SWARM

In this section, finite-time formation control problem with time-delay and input saturation is investigated. First, by using precise feedback linearization, the system (1) is transformed into a linear system. Since only the UAV directly connected to the leader UAV can receive the leader's states, a fixed-time observer is constructed for each follower UAV to estimate the leader's states. Then, Artstein's transformation is introduced to transform the delayed system into a delay-free system and a distributed control protocol is proposed to solve finite-time formation control problem with input saturation and time-delay.

The model of UAV can be rewritten as

$$\dot{\varphi}_i = f(\varphi_i) + c(\varphi_i)\eta_i(t - \tau_i), \tag{3}$$

where $\varphi_i = (x_i, y_i, z_i, V_i, \theta_i, \psi_i)^T$, $\eta_i = (\eta_{xi}, \eta_{yi}, \eta_{zi})^T$,

$$f(\varphi_i) = \begin{bmatrix} V_i\cos\theta_i\cos\psi_i \\ V_i\sin\theta_i \\ -V_i\cos\theta_i\sin\psi_i \\ -g\sin\theta_i \\ -\frac{g}{V_i}\cos\theta_i \\ 0 \end{bmatrix}, \quad c(\varphi_i) = \begin{bmatrix} 0 & 0 & 0 \\ 0 & 0 & 0 \\ 0 & 0 & 0 \\ g & 0 & 0 \\ 0 & \frac{g}{V_i} & 0 \\ 0 & 0 & \frac{-g}{V_i\cos\theta_i} \end{bmatrix}.$$

By using precise feedback linearization [8], the system (3) can be transformed into the following linear system

$$\dot{\zeta}_i = A\zeta_i + Bu_i(t - \tau_i), \tag{4}$$

where $\zeta_i = (x_i, y_i, z_i, \dot{x}_i, \dot{y}_i, \dot{z}_i)^T$, $A = \begin{pmatrix} 0_{3\times3} & I_{3\times3} \\ 0_{3\times3} & 0_{3\times3} \end{pmatrix}$, $B = \begin{pmatrix} 0_{3\times3} \\ I_{3\times3} \end{pmatrix}$.

The state feedback transformation can be specified by

$$u_i(t - \tau_i) = \begin{pmatrix} 0 \\ -g \\ 0 \end{pmatrix} + \Gamma(\theta_i, \varphi_i)\begin{pmatrix} \eta_{xi}(t - \tau_i) \\ \eta_{yi}(t - \tau_i) \\ \eta_{zi}(t - \tau_i) \end{pmatrix}, \tag{5}$$

where Γ is the transformation matrix and $\Gamma(\theta_i, \varphi_i) = \begin{bmatrix} g\cos\theta_i\cos\psi_i & -g\sin\theta_i\cos\psi_i & g\sin\psi_i \\ g\sin\theta_i & g\cos\theta_i & 0 \\ -g\cos\theta_i\sin\psi_i & g\sin\theta_i\sin\psi_i & g\cos\psi_i \end{bmatrix}$.

With $p_i = (x_i, y_i, z_i)^T$, (4) can be expressed as the following second-order system

$$\ddot{p}_i = u_i(t - \tau_i), \tag{6}$$

where $p_i \in R^3$, $u_i \in R^3$ denote the position, control input, respectively, $i = 1, 2, \cdots, N$.

$$\ddot{p}_0(t) = u_0(t), \tag{7}$$

where $p_0 \in R^3$, $u_0 \in R^3$ denote the position, control input of leader UAV, respectively. The control input should not exceed the limitation of the actuator, that is, $\|u_0\| < \rho$, ρ is an appropriate positive constant.

Since only the UAV directly connected to the leader UAV can receive the leader's states, distributed observer is constructed for each follower UAV. In order to estimate the leader's states quickly and accurately, fixed-time stability theory was introduced [36], [37], and the fixed-time observer is designed as follows:

$$\dot{\hat{p}}_i = \frac{\sum_{j=0}^{N} a_{ij}\dot{\hat{p}}_j}{\sum_{j=0}^{N} a_{ij}} - \frac{\alpha}{\sum_{j=0}^{N} a_{ij}} sig\left(\sum_{j=0}^{N} a_{ij}(\hat{p}_i - \hat{p}_j)\right)^{m/n} - \frac{\beta}{\sum_{j=0}^{N} a_{ij}} sig\left(\sum_{j=0}^{N} a_{ij}(\hat{p}_i - \hat{p}_j)\right)^{c/d}, \tag{8}$$

where α, β denote observer gains and $\alpha, \beta > 0$, m, n, c, d are positive odd integers satisfying $m > n$ and $c < d$, $\hat{p}_i$ is the estimate of observer for the ith UAV, $\hat{p}_0 = p_0$.

Theorem 1: Suppose that the graph for the follower UAVs is connected, and there is at least one UAV that can directly obtain the leader's information. The fixed-time observer (8) *can estimate the leader's states in fixed-time and the settling time is bounded by*

$$T_1 < \frac{1}{\alpha}\frac{n}{m-n} + \frac{1}{\beta}\frac{d}{d-c}.$$

Proof:

Define $\phi_i = \sum_{j=1}^{N} a_{ij}(\hat{p}_i - \hat{p}_j) + a_{i0}(\hat{p}_i - p_0)$, (8) can be rewritten as

$$\dot{\phi}_i = -\alpha sig(\phi_i)^{m/n} - \beta sig(\phi_i)^{c/d}. \tag{9}$$

Choose the Lyapunov function candidate $V_1(t) = \frac{1}{2}\phi^T\phi$, where $\phi = (\phi_1^T, \phi_2^T, \cdots, \phi_N^T)^T$, $\phi_i = (\phi_{i1}, \phi_{i2}, \phi_{i3})^T$. According to the definition of $sig(\bullet)^\gamma$, we have $sig(\phi_i)^\gamma = \left[sig(\phi_{i1})^\gamma, sig(\phi_{i2})^\gamma, sig(\phi_{i3})^\gamma\right]^T$. Then, we have $\phi_i^T sig(\phi_i)^{m/n} = \sum_{j=1}^{3}|\phi_{ij}|^{m/n+1}$, $\phi_i^T sig(\phi_i)^{c/d} = \sum_{j=1}^{3}|\phi_{ij}|^{c/d+1}$. From Lemma 3, we can obtain that $\sum_{i=1}^{N}\sum_{j=1}^{3}|\phi_{ij}|^{m/n+1} \geq \left(\sum_{i=1}^{N}\sum_{j=1}^{3}|\phi_{ij}|^2\right)^{\frac{m/n+1}{2}} = \|\phi\|^{m/n+1}$, $\sum_{i=1}^{N}\sum_{j=1}^{3}|\phi_{ij}|^{c/d+1} \geq \|\phi\|^{c/d+1}$. Taking the derivative of $V_1(t)$, it follows that

$$\dot{V}_1(t) = -\alpha\sum_{i=1}^{N}\phi_i^T sig(\phi_i)^{m/n} - \beta\sum_{i=1}^{N}\phi_i^T sig(\phi_i)^{c/d}$$

$$
\begin{aligned}
&= -\alpha \sum_{i=1}^{N}\sum_{j=1}^{3} \left|\phi_{ij}\right|^{m/n+1} - \beta \sum_{i=1}^{N}\sum_{j=1}^{3} \left|\phi_{ij}\right|^{c/d+1} \\
&= -\alpha \sum_{i=1}^{N}\sum_{j=1}^{3} \left(\phi_{ij}^2\right)^{\frac{m/n+1}{2}} - \beta \sum_{i=1}^{N}\sum_{j=1}^{3} \left(\phi_{ij}^2\right)^{\frac{c/d+1}{2}} \\
&\le -\alpha \left(\sum_{i=1}^{N}\sum_{j=1}^{3} \phi_{ij}^2\right)^{\frac{m/n+1}{2}} - \beta \left(\sum_{i=1}^{N}\sum_{j=1}^{3} \phi_{ij}^2\right)^{\frac{c/d+1}{2}} \\
&= -\alpha \left(\|\phi\|^2\right)^{\frac{m/n+1}{2}} - \beta \left(\|\phi\|^2\right)^{\frac{c/d+1}{2}} \\
&= -\alpha \|\phi\|^{m/n+1} - \beta \|\phi\|^{c/d+1} \\
&= -\alpha 2^{\frac{m/n+1}{2}} V_1^{\frac{m/n+1}{2}}(t) - \beta 2^{\frac{c/d+1}{2}} V_1^{\frac{c/d+1}{2}}(t). \qquad (10)
\end{aligned}
$$

Define $\chi_1 = \sqrt{2V_1(t)}$, it follows that

$$\dot{\chi}_1 \le -\alpha \chi_1^{m/n} - \beta \chi_1^{c/d}. \qquad (11)$$

It follows from Lemma 2 that $\phi_i = 0_3$ within fixed-time and the fixed-time upper bound can be computed as $T_1 < \frac{1}{\alpha}\frac{n}{m-n} + \frac{1}{\beta}\frac{d}{d-c}$. Then we can obtain $\|\phi\| = \left\|((L+H)\otimes I_3)\left(\hat{p} - 1_N \otimes p_0\right)\right\| = 0$ when $t \ge T_1$, $\hat{p} = \left[\hat{p}_1^T, \hat{p}_2^T, \cdots, \hat{p}_N^T\right]^T$. Noting that the graph for the follower UAVs is connected, and there is at least one UAV that can directly obtain the leader's information. According to Lemma 4, $L+H$ is positive definite and symmetric, and we get $\left\|\hat{p} - 1_N \otimes p_0\right\| = 0$, $\forall t \ge T_1$, which means $\hat{p}_1 = \hat{p}_2 = \cdots = \hat{p}_N = p_0$, when $t \ge T_1$. This is the end of proof. □

Remark 1: From Theorem 1, we can obtain that $\hat{p}_1 = \hat{p}_2 = \cdots = \hat{p}_N = p_0$, *when* $t \ge T_1$. *Similar to* (8), *we design a fixed-time observer to estimate* $\dot{p}_0$, *that is,* $\ddot{\hat{p}}_i = \frac{\sum_{j=0}^{N} a_{ij}\ddot{\hat{p}}_j}{\sum_{j=0}^{N} a_{ij}} - \frac{\alpha}{\sum_{j=0}^{N} a_{ij}} sig\left(\sum_{j=0}^{N} a_{ij}\left(\dot{\hat{p}}_i - \dot{\hat{p}}_j\right)\right)^{m/n} - \frac{\beta}{\sum_{j=0}^{N} a_{ij}} sig\left(\sum_{j=0}^{N} a_{ij}\left(\dot{\hat{p}}_i - \dot{\hat{p}}_j\right)\right)^{c/d}$. *By using the same proof process as Theorem 1, we can prove that* $\dot{\hat{p}}_1 = \dot{\hat{p}}_2 = \cdots = \dot{\hat{p}}_N = \dot{p}_0$, *when* $t \ge T_1$.

Considering the time-delay, the leader's information received by the ith UAV is lagging, and the lag time is τ_i. Therefore, at time t, the control input of each UAV is determined by the states of time $t - \tau_i$. Then, all follower UAVs can track the lag items of the leader UAV. As shown in [32], [38], and [39], define the state tracking errors $\varepsilon_{pi} = p_i(t) - p_0(t-\tau_i)$, $\varepsilon_{\dot{p}i} = \dot{p}_i(t) - \dot{p}_0(t-\tau_i)$, where $\dot{p}_i = [V_i \cos\theta_i \cos\psi_i, V_i \sin\theta_i, -V_i \cos\theta_i \sin\psi_i]^T$. The time-delay second-order system (6) (7) can be written as

$$\begin{cases} \dot{\varepsilon}_{pi} = \varepsilon_{\dot{p}i} \\ \dot{\varepsilon}_{\dot{p}i} = u_i(t-\tau_i) - u_0(t-\tau_i). \end{cases} \qquad (12)$$

Artstein's transformation [31] is introduced to transform the delayed system (12) into a delay-free system. Then we have

$$\begin{cases} y_{1i} = \varepsilon_{pi} + \int_{-\tau_i}^{0} (-\tau_i - s)\left(u_i(t+s) - u_0(t+s)\right) ds \\ y_{2i} = \varepsilon_{\dot{p}i} + \int_{-\tau_i}^{0} \left(u_i(t+s) - u_0(t+s)\right) ds. \end{cases} \qquad (13)$$

After transformation, we have

$$\begin{cases} \dot{y}_{1i} = y_{2i} - \tau_i\left(u_i(t) - u_0(t)\right) \\ \dot{y}_{2i} = u_i(t) - u_0(t). \end{cases} \qquad (14)$$

To tackle the input saturation problem, the following saturation function is introduced by

$$s_\gamma^\alpha(x) = \begin{cases} sig(x)^\alpha, & |x| < \gamma \\ \dfrac{\gamma^\alpha sig(x)^\alpha}{|x|^\alpha}, & |x| \ge \gamma. \end{cases} \qquad (15)$$

where α is a positive constant, $\gamma > 0$ is the design parameter, $x \in R$. In addition, $s_\gamma^\alpha(X) = \left[s_\gamma^\alpha(x_1), s_\gamma^\alpha(x_2), \cdots, s_\gamma^\alpha(x_n)\right]^T$, $X = [x_1, x_2, \cdots, x_n]^T$.

From [18], the following function is specified by

$$S_\gamma^\alpha(x) = \begin{cases} \dfrac{|x|^{\alpha+1}}{\alpha+1}, & |x| < \gamma \\ \gamma^\alpha |x| - \dfrac{\alpha\gamma^{\alpha+1}}{\alpha+1}, & |x| \ge \gamma. \end{cases} \qquad (16)$$

$S_\gamma^\alpha(x)$ is radially unbounded and positive definite. Taking the time derivative of $S_\gamma^\alpha(x)$, we obtain that $\frac{dS_\gamma^\alpha(x)}{dt} = s_\gamma^\alpha(x)$. In addition, $S_\gamma^\alpha(X) = \left[S_\gamma^\alpha(x_1), S_\gamma^\alpha(x_2), \cdots, S_\gamma^\alpha(x_n)\right]^T$, $X = [x_1, x_2, \cdots, x_n]^T$.

For UAV swarm system, finite-time formation control protocol with time-delay and input saturation is designed as follows.

$$\begin{pmatrix} \eta_{xi}(t-\tau_i) \\ \eta_{yi}(t-\tau_i) \\ \eta_{zi}(t-\tau_i) \end{pmatrix} = \Gamma(\theta_i, \varphi_i)^{-1} \begin{pmatrix} u_{ix}(t-\tau_i) \\ u_{iy}(t-\tau_i) + g \\ u_{iz}(t-\tau_i) \end{pmatrix}, \qquad (17)$$

$$
\begin{aligned}
\begin{pmatrix} u_{ix}(t) \\ u_{iy}(t) \\ u_{iz}(t) \end{pmatrix} &= s_{\gamma_2}^1\left(\ddot{\hat{p}}_i\right) - k_1 s_{\gamma_1}^{\alpha_1}\left(\sum_{j=1}^{N} a_{ij}\left(\left(y_{1i} - y_{1j} - r_{ij}\right)\right.\right. \\
&\quad \left.\left. + \tau_i\left(y_{2i} - y_{2j}\right)\right) + a_{i0}\left(y_{1i} - r_i + \tau_i y_{2i}\right)\right) \\
&\quad - k_2 s_{\gamma_1}^{\alpha_2}\left(\sum_{j=1}^{N} a_{ij}\left(y_{2i} - y_{2j}\right) + a_{i0} y_{2i}\right), \qquad (18)
\end{aligned}
$$

where $\Gamma(\theta_i, \varphi_i)$ is defined in (5), $\gamma_1 > 0$, $\gamma_2 = \max\left\{|u_{0x}|, |u_{0y}|, |u_{0z}|\right\}$, $k_1 > 0$, $k_2 > 0$, $\alpha_1 \in (0,1)$, $\alpha_2 = \frac{2\alpha_1}{1+\alpha_1}$, r_i, r_{ij} are the relative position vectors and $r_{ij} = r_i - r_j$.

Remark 2: From Theorem 1 and Remark 1, we can obtain that when $t \ge T_1$, *the observer can stably estimate the leader's states, that is* $\hat{p}_1 = \hat{p}_2 = \cdots = \hat{p}_N = p_0$, $\dot{\hat{p}}_1 = \dot{\hat{p}}_2 = \cdots = \dot{\hat{p}}_N = \dot{p}_0$. *Using the control protocol* (18), *the ith UAV's controller receives the states of its neighbors to calculate its control input continuously and stores its control input on interval* $[t-\tau_i, t]$. *Then, the ith UAV's controller converts the control input* u_i *into the control input* η_i *of the actuator*

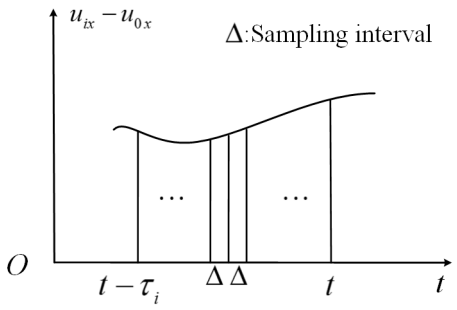

FIGURE 2. Schematic diagram of $u_{ix} - u_{0x}$.

by using (17). *Meanwhile, the ith UAV's controller stores the history values of observer's output on interval* $[t-\tau_i, t]$ *to calculate the Artstein's transformation (13) and broadcasts its Artstein's transformation states* y_{1i}, y_{2i}. *A uniform robust exact differentiator [40] can accurately calculate the derivative of* $\dot{p}_0$, *i.e.* u_0.

Remark 3: From (7), *each UAV needs to store the history values of observer's output and its control input* u_i *on interval* $[t-\tau_i, t]$ *to calculate the Artstein's transformation* (13). *The Artstein's transformation* (13) *involves integral terms* $\int_{-\tau_i}^{0}(u_i(t+s)-u_0(t+s))\,ds$ *and* $\int_{-\tau_i}^{0}(-\tau_i-s)(u_i(t+s)-u_0(t+s))\,ds$. *There are two ways to implement the integral term in practical application. First, the Newton-Cotts formula [41] can be used to approximate the integral precisely, which is a numerical integration method. With electronic computing equipment, numerical integration can calculate integrals quickly and efficiently. Assume that the sampling interval is* Δ *and the schematic diagram of* $u_{ix}-u_{0x}$ *is shown in Figure 2 on interval* $[t-\tau_i, t]$. *By using Newton-Cotts formula, we can obtain that* $\int_{-\tau_i}^{0}(u_{ix}(t+s)-u_{0x}(t+s))\,ds = \frac{1}{2}\sum_{l=1}^{\tau_i/\Delta}\Delta[(u_{ix}(t-\tau_i+(l-1)\Delta)-u_{0x}(t-\tau_i+(l-1)\Delta)) + (u_{ix}(t-\tau_i+l\Delta)-u_{0x}(t-\tau_i+l\Delta))]$. *The integral is approximated by the sum of the areas of all trapezoids. Second, the design and application of controllers can be achieved by using Simulink and Real-Time Workshop (RTW). This method firstly designs the controller and sets the simulation step size in Simulink, and then uses the RTW module to generate the corresponding code or executable file of the target system. RTW provides a direct way from controller model design to hardware implementation.*

Remark 4: It is worth mentioning that the formation control protocol contains the component $s_{\gamma_2}^{1}\left(\ddot{\hat{p}}_i\right)$. *When* $t < T_1$, $s_{\gamma_2}^{1}\left(\ddot{p}_i\right)$ *guarantees that the control inputs have an upper bound. From* $\|u_0\| < \rho$, *we can get* $s_{\gamma_3}^{1}\left(\ddot{\hat{p}}_i\right) = u_0$ *by choosing* $\gamma_2 = \max\left\{|u_{0x}|, |u_{0y}|, |u_{0z}|\right\}$ *when* $t > T_1$.

In this method, we design the finite-time control protocol on the basis of Artstein's transformation and saturation function, which is fully distributed using the finite-time observer. First, we show that the finite-time formation control protocol is bounded and the upper bound is given as follows:

$$\begin{aligned}\|u_i\| &= \sqrt{u_{ix}^2+u_{iy}^2+u_{iz}^2}\\ &= \Bigg\| s_{\gamma_2}^{1}\left(\ddot{\hat{p}}_i\right) - k_1 s_{\gamma_1}^{\alpha_1}\left(\sum_{j=1}^{N} a_{ij}\left(\left(y_{1i}-y_{1j}-r_{ij}\right)\right.\right.\\ &\quad \left.+\tau_i\left(y_{2i}-y_{2j}\right)\right)+a_{i0}\left(y_{1i}-r_i+\tau_i y_{2i}\right)\Bigg)\\ &\quad -k_2 s_{\gamma_1}^{\alpha_2}\left(\sum_{j=1}^{N} a_{ij}\left(y_{2i}-y_{2j}\right)+a_{i0}y_{2i}\right)\Bigg\|\\ &\le \sqrt{3}k_1\gamma_1^{\alpha_1}+\sqrt{3}k_2\gamma_1^{\alpha_2}+\sqrt{3}\gamma_2 = \|u_{\max}\|. \end{aligned} \quad (19)$$

Noting that the control parameters determine the upper bound of control input, which can tackle the control input saturation prolems of UAVs. For practical UAV actuator, we can adjust the parameters of control protocol (18) to satisfy the input saturation constraint.

Theorem 2: Consider UAV swarm system composed of N UAVs (called followers) and a leader UAV. Suppose that the communication topology is connected, and there is at least one UAV that can directly obtain the leader's information. With the formation control protocols (17) (18), *finite-time formation control problem with time-delay and input saturation can be solved if the control parameters are appropriately selected as* $\alpha_1 \in (0,1)$, $\alpha_2 = \frac{2\alpha_1}{1+\alpha_1}$, $k_1 > 0$, $k_2 > 0$, $\gamma_2 = \max\left\{|u_{0x}|, |u_{0y}|, |u_{0z}|\right\}$. *In addition,* γ_1 *can be selected according to the limitation of the actuator.*

Proof: According to Lemma 5, we introduce Artstein's transformation to transform the delayed system (12). Therefore, we only need to prove that the system (14) is finite-time stabilizable by control protocol (18), then the system (12) is finite-time stabilizable by the control protocol (18) and Artstein's transformation (13).

Define the formation control errors for the *i*th UAV as

$$\begin{aligned} e_i &= \sum_{j=1}^{N} a_{ij}\left(\left(y_{1i}-y_{1j}-r_{ij}\right)+\tau_i\left(y_{2i}-y_{2j}\right)\right)\\ &\quad +a_{i0}\left(y_{1i}-r_i+\tau_i y_{2i}\right), \end{aligned} \quad (20)$$

$$g_i = \sum_{j=1}^{N} a_{ij}\left(y_{2i}-y_{2j}\right)+a_{i0}y_{2i}. \quad (21)$$

From Theorem 1, we can get $\ddot{\hat{p}}_i = u_0$ when $t > T_1$. Define $\bar{u}_i = u_i - u_0$, then we have $\dot{y}_{2i} = \bar{u}_i(t) = -k_1 s_{\gamma_1}^{\alpha_1}(e_i) - k_2 s_{\gamma_1}^{\alpha_2}(g_i)$, which leads to the following formation control error system.

$$\begin{aligned} \dot{e}_i &= g_i\\ \dot{g}_i &= -k_1\left(\sum_{j=1}^{N} a_{ij}\left(s_{\gamma_1}^{\alpha_1}(e_i)-s_{\gamma_1}^{\alpha_1}\left(e_j\right)\right)+a_{i0}s_{\gamma_1}^{\alpha_1}(e_i)\right)\\ &\quad -k_2\left(\sum_{j=1}^{N} a_{ij}\left(s_{\gamma_1}^{\alpha_2}(g_i)-s_{\gamma_1}^{\alpha_2}\left(g_j\right)\right)+a_{i0}s_{\gamma_1}^{\alpha_2}(g_i)\right). \end{aligned} \quad (22)$$

In what follows, the proof is divided into two steps: First, we prove that error system (22) is globally asymptotically stable. Then, we will prove that error system (22) is globally finite-time stable.

First, define $E = \left[e_1^T, e_2^T, \cdots, e_N^T\right]^T$, $G = \left[g_1^T, g_2^T, \cdots, g_N^T\right]^T$, consider the following Lyapunov function candidate

$$V_2(t) = k_1 \sum_{i=1}^{N} S_{\gamma_1}^{\alpha_1}(e_i) + \frac{1}{2} G^T \left((L+H)^{-1} \otimes I_3\right) G. \quad (23)$$

From [18], $S_{\gamma_1}^{\alpha_1}(x)$ is radially unbounded and positive definite. It follows from Lemma 4 that $L + H$ is positive definite and symmetric. Then, we can obtain that $V_2(t)$ is radially unbounded and globally positive definite.

The time derivative of $V_2(t)$ along (22) is

$$\begin{aligned}
\dot{V}_2(t) &= k_1 \sum_{i=1}^{N} \dot{e}_i^T s_{\gamma_1}^{\alpha_1}(e_i) + G^T \left((L+H)^{-1} \otimes I_3\right) \dot{G} \\
&= k_1 \sum_{i=1}^{N} g_i^T s_{\gamma_1}^{\alpha_1}(e_i) + G^T \left(-k_1 s_{\gamma_1}^{\alpha_1}(E) - k_2 s_{\gamma_1}^{\alpha_2}(G)\right) \\
&= k_1 \sum_{i=1}^{N} g_i^T s_{\gamma_1}^{\alpha_1}(e_i) - k_1 G^T s_{\gamma_1}^{\alpha_1}(E) \\
&\quad - k_2 \sum_{i=1}^{N} g_i^T s_{\gamma_1}^{\alpha_2}(g_i) \\
&= -k_2 \sum_{i=1}^{N} g_i^T s_{\gamma_1}^{\alpha_2}(g_i). \qquad (24)
\end{aligned}$$

By the definition of saturation function $s_\gamma^\alpha(x)$, we get

$$-k_2 \sum_{i=1}^{N} g_i^T s_{\gamma_1}^{\alpha_2}(g_i) = \begin{cases} -k_2 \sum\limits_{i=1}^{N} \sum\limits_{j=1}^{3} |g_{ij}|^{\alpha_2+1}, & |g_{ij}| < \gamma_1 \\ -k_2 \sum\limits_{i=1}^{N} \sum\limits_{j=1}^{3} \gamma_1^{\alpha_2} |g_{ij}|, & |g_{ij}| \geq \gamma_1. \end{cases} \quad (25)$$

From (25) we obtain that $\dot{V}_2(t) \leq 0$ and $V_2(t)$ is non-increasing. By LaSalle's invariance principle, it is concluded that $\left(E^T, G^T\right)^T$ will converge to the set $\left\{\left(E^T, G^T\right)^T \mid \dot{V}_2(t) \equiv 0\right\}$ as $t \to \infty$. $\dot{V}_2(t) \equiv 0$ together with (25) means $g_i \equiv 0_3$, and further $\dot{g}_i \equiv 0_3$, $e_i \equiv 0_3$ from (22), which implies that the equilibrium $\left(e_i^T, g_i^T\right)^T = 0_6$ of system (22) is globally asymptotically stable.

Next, it will be proved that the error system (22) is globally finite-time stable.

Owing to $\dot{V}_2(t) \leq 0$, we obtain that $V_2(t) \leq V_2(0)$ and the control errors e_i, g_i are all bounded for $t > 0$. When $|e_{ij}| \geq \gamma_1$ and $|g_{ij}| \geq \gamma_1, j = 1, 2, 3$, we will show that the control errors e_i, g_i converge to the region $|e_{ij}| < \gamma_1$ and $|g_{ij}| < \gamma_1$ in finite time. Then, the error system (22) can be rewritten as

$$\begin{aligned}
\dot{e}_i &= g_i \\
\dot{g}_i &= -k_1 \left(\sum_{j=1}^{N} a_{ij} \gamma_1^{\alpha_1} \left(sgn(e_i) - sgn\left(e_j\right)\right) + a_{i0} sgn(e_i) \right) \\
&\quad - k_2 \left(\sum_{j=1}^{N} a_{ij} \gamma_1^{\alpha_2} \left(sgn(g_i) - sgn\left(g_j\right)\right) + a_{i0} sgn(g_i) \right).
\end{aligned} \quad (26)$$

By Definition 1, the system (26) is homogeneous with negative degree $k = -1$ with respect to $(2, 2, 2, 1, 1, 1)$. It follows from Lemma 1 that the system (26) is local finite-time stable. From (25), we have

$$\dot{V}_2(t) = -k_2 \sum_{i=1}^{N} \sum_{j=1}^{3} \gamma_1^{\alpha_2} |g_{ij}| \leq 0, \quad |g_{ij}| \geq \gamma_1, \quad (27)$$

which implies that the system (26) is globally asymptotically stable. Then, we can obtain that the errors e_i and g_i of system (26) converge to 0_3 in finite time. It is easily inferred that the control errors converge to the region $|e_{ij}| < \gamma_1, |g_{ij}| < \gamma_1$ in finite time and stay the region forever. From (27), we have

$$\begin{aligned}
\dot{V}_2(t) &= -k_2 \sum_{i=1}^{N} \sum_{j=1}^{3} \gamma_1^{\alpha_2} |g_{ij}| = -k_2 \gamma_1^{\alpha_2} \sum_{i=1}^{N} \sum_{j=1}^{3} |g_{ij}|^{2 \times \frac{1}{2}} \\
&\leq -k_2 \gamma_1^{\alpha_2} \left(\sum_{i=1}^{N} \sum_{j=1}^{3} |g_{ij}|^2 \right)^{\frac{1}{2}} = -k_2 \gamma_1^{\alpha_2} \|G\|. \qquad (28)
\end{aligned}$$

It follows from Theorem 3 [42] that $V_2(t)$ of the system (26) is homogeneous with degree $l = 2$. Note that the system (26) is homogeneous with negative degree $k = -1$, by using [43, Lemma 2] and [44, Proposition 2.3], we can obtain that

$$\dot{V}_2(t) \leq \left(- \min_{\{G: V_2 = 1\}} \left(k_2 \gamma_1^{\alpha_2} \|G\|\right) \right) V_2^{\frac{l+k}{l}} = -\Delta_1 V_2^{\frac{1}{2}}(t). \quad (29)$$

where $\Delta_1 = \min\limits_{\{G: V_2 = 1\}} \left(k_2 \gamma_1^{\alpha_2} \|G\|\right)$. It follows from [44, Th. 3] that the control errors converge to the region $|e_{ij}| < \gamma_1$, $|g_{ij}| < \gamma_1$ with the settling time $T_2 \leq \frac{2\sqrt{V_2(0)}}{\Delta_1}$.

Then, error system (22) becomes

$$\begin{aligned}
\dot{e}_i &= g_i \\
\dot{g}_i &= -k_1 \left(\sum_{j=1}^{N} a_{ij} \left(sig(e_i)^{\alpha_1} - sig\left(e_j\right)^{\alpha_1}\right) + a_{i0} sig(e_i)^{\alpha_1} \right) \\
&\quad - k_2 \left(\sum_{j=1}^{N} a_{ij} \left(sig(g_i)^{\alpha_2} - sig\left(g_j\right)^{\alpha_2}\right) + a_{i0} sig(g_i)^{\alpha_2} \right).
\end{aligned} \quad (30)$$

By Definition 1, the system (30) is homogeneous with negative degree $\alpha_2 - 1$ with respect to $(\frac{2}{1+\alpha_1}, \frac{2}{1+\alpha_1}, \frac{2}{1+\alpha_1}, 1, 1, 1)$.

It follows from Lemma 1 that the system (30) is local finite-time stable. From (25), we have

$$\dot{V}_2(t) = -k_2 \sum_{i=1}^{N} \sum_{j=1}^{3} \left|g_{ij}\right|^{\alpha_2+1} \leq 0, \left|g_{ij}\right| < \gamma_1. \quad (31)$$

which implies that the system (30) is globally asymptotically stable. It can be concluded that the system (30) is globally finite-time stable. From (31), we have

$$\begin{aligned}\dot{V}_2(t) &= -k_2 \sum_{i=1}^{N} \sum_{j=1}^{3} \left|g_{ij}\right|^{\alpha_2+1} \\ &\leq -k_2 \left(\sum_{i=1}^{N} \sum_{j=1}^{3} g_{ij}^2 \right)^{\frac{\alpha_2+1}{2}} = -k_2 \|G\|^{\alpha_2+1}. \end{aligned} \quad (32)$$

Similarly, we have

$$\begin{aligned}\dot{V}_2(t) &\leq \left(- \min_{\{G:V_2=1\}} \left(k_2 \|G\|^{\alpha_2+1} \right) \right) V_2^{\frac{2+(\alpha_2-1)}{2}}(t) \\ &= -\Delta_2 V_2^{\frac{\alpha_2+1}{2}}(t). \end{aligned} \quad (33)$$

where $\Delta_2 = \min_{\{G:V_2=1\}} \left(k_2 \|G\|^{\alpha_2+1} \right)$. Then, the system (30) is globally finite-time stable with the settling time $T_3 \leq \frac{2\sqrt{V_2^{1-\alpha_2}(0)}}{\Delta_2(1-\alpha_2)}$.

As a result, error system (22) is globally finite-time stable with the settling time $T_2 + T_3 \leq \frac{2\sqrt{V_2(0)}}{\Delta_1} + \frac{2\sqrt{V_2^{1-\alpha_2}(0)}}{\Delta_2(1-\alpha_2)}$. From (20) (21), we have $\|G\| = \|((L+H) \otimes I_3) Y_2\| = 0$ and $\|E\| = \|((L+H) \otimes I_3)(Y_1 - r + (\tau \otimes I_3) Y_2)\| = 0$, when $\forall t \geq \frac{1}{\alpha}\frac{n}{m-n} + \frac{1}{\beta}\frac{d}{d-c} + \frac{2\sqrt{V_2(0)}}{\Delta_1} + \frac{2\sqrt{V_2^{1-\alpha_2}(0)}}{\Delta_2(1-\alpha_2)}$, where $Y_1 = \left(y_{11}^T, y_{12}^T, \cdots, y_{1N}^T\right)^T$, $Y_2 = \left(y_{21}^T, y_{22}^T, \cdots, y_{2N}^T\right)^T$, $r = \left(r_1^T, r_2^T, \cdots, r_N^T\right)^T$, $\tau = diag(\tau_1, \tau_2, \cdots, \tau_N)$. According to Lemma 4, $L + H$ is positive definite and symmetric, and we get $y_{1i} - r_i = 0_3, y_{2i} = 0_3, \forall t \geq \frac{1}{\alpha}\frac{n}{m-n} + \frac{1}{\beta}\frac{d}{d-c} + \frac{2\sqrt{V_2(0)}}{\Delta_1} + \frac{2\sqrt{V_2^{1-\alpha_2}(0)}}{\Delta_2(1-\alpha_2)}$. It follows from Artstein's transformation (13) that $\int_{-\tau_i}^{0} (u_i(t+s) - u_0(t+s))\, ds$ converges to 0 with the settling time $T = T_1 + T_2 + T_3 + \max\{\tau_i\} \leq \frac{1}{\alpha}\frac{n}{m-n} + \frac{1}{\beta}\frac{d}{d-c} + \frac{2\sqrt{V_2(0)}}{\Delta_1} + \frac{2\sqrt{V_2^{1-\alpha_2}(0)}}{\Delta_2(1-\alpha_2)} + \max\{\tau_i\}$. We can obtain that the transformation system (14) is finite-time stable with the control protocol (18). Therefore, according to Lemma 5, the time-delay system (6) is finite-time stable with the control protocol (18) and Artstein's transformation (13). We can conclude that the finite-time formation control problem for UAV swarm with time-delay and input saturation can be solved with distributed control protocols (17) (18). This is the end of proof. □

Remark 5: In this section, we discuss finite-time formation control problem with constant time-delay and input saturation. However, the delay caused by UAV processing and communication may be unknown constant and time-varying. Then, the time-delay estimation method presented in [45] and [46] can be used to estimate the unknown constant time-delay. During the flight of each UAV, the controller needs to operate within a certain time range to ensure the flight safety of the UAV, which is called acceptable time. Therefore, the time-delay needs to be bounded such that the operation does not affect flight safety. For non-identical time-varying delays, we can consider the upper bound of the delays that exist in all UAVs, as shown in [47]. In summary, the proposed control protocol can be extended to the finite-time formation control problem with unknown constant delays and time-varying delays.

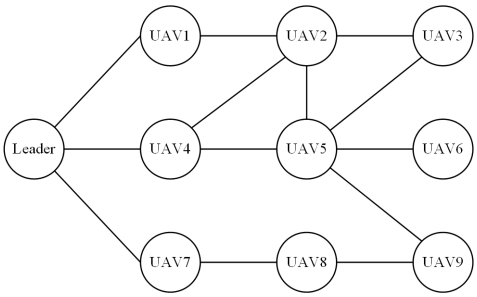

FIGURE 3. The communication topology between UAVs.

TABLE 1. The initial conditions of UAV swarm.

States	x_i/m	y_i/m	z_i/m	V_i/m/s	$\theta_i/^\circ$	$\psi_i/^\circ$
UAV1	450	134	260	85	5.5	4.8
UAV2	310	110	195	70	4.9	-3.1
UAV3	305	98	420	88.5	-2.8	3.6
UAV4	155	46	96	78	-3.5	2.8
UAV5	167	53	510	84	2.8	4.6
UAV6	10	10	7	71	-3.5	-2.6
UAV7	5	13	180	73	3	2
UAV8	3	15	400	68	4.5	-3.6
UAV9	5	10	580	89	3.8	4
Leader	240	75	300	80	0	0

IV. SIMULATION RESULTS

To verify the validity of finite-time formation control protocol, we give a simulation example on UAV swarm to maintain the formation shape. Consider a UAV swarm system consisting of a leader UAV and nine follower UAVs. The communication topology between UAVs is shown in Figure 3. The trajectory of the leader is specified by

$$\begin{cases} V_0 = 80 + 8\sin(0.16t) \\ \theta_0 = 0.12 sin(0.04t) \\ \psi_0 = 0.02\sin(0.1t). \end{cases} \quad (34)$$

The initial conditions for UAV swarm are set according to Table 1. The desired formation vectors are given by $r_1 = \left(240\ 75\ 0\right)^T$, $r_2 = \left(80\ 25\ -100\right)^T$, $r_3 = \left(80\ 25\ 100\right)^T$, $r_4 = \left(-80\ -25\ -200\right)^T$, $r_5 = \left(-80\ -25\ 200\right)^T$, $r_6 = \left(-240\ -75\ -300\right)^T$, $r_7 = \left(-240\ -75\ -100\right)^T$, $r_8 = \left(-240\ -75\ 100\right)^T$, $r_9 = \left(-240\ -75\ 300\right)^T$, where the unit is m.

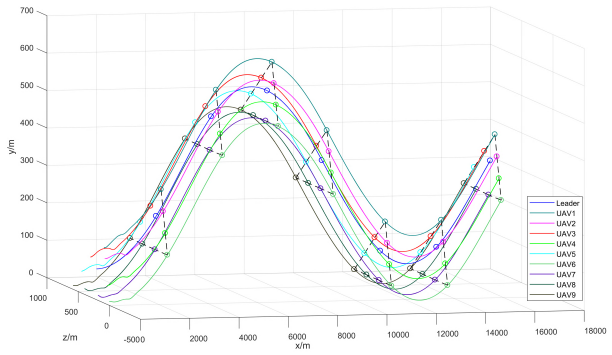

FIGURE 4. The trajectories of UAV swarm formation flight.

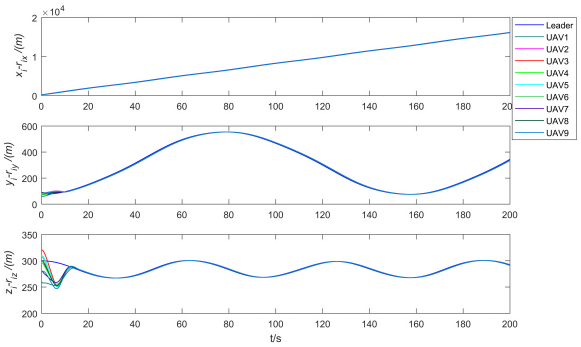

FIGURE 5. Position tracking of all followers.

Assume that the limitation of the actuator is $70m/s^2$, which means the control input $\|u_i\| \leq 70m/s^2$. The observer parameters are chosen as $\alpha = 5$, $\beta = 4.5$, $m = 7$, $n = 5$, $c = 5$, $d = 7$. The formation controller parameters are chosen as $\alpha_1 = 0.6$, $\alpha_2 = 0.75$, $k_1 = 5$, $k_2 = 5$, $\gamma_1 = 7$, $\gamma_2 = 1.4$. Time-delays are chosen as $\tau_1 = \tau_2 = \tau_3 = 0.6s$, $\tau_4 = \tau_5 = \tau_6 = 0.8s$, $\tau_7 = \tau_8 = \tau_9 = 1s$. It follows from (19) that $\|u_i\| \leq \sqrt{3}k_1\gamma_1^{\alpha_1} + \sqrt{3}k_2\gamma_1^{\alpha_2} + \sqrt{3}\gamma_2 = 67.52m/s^2$, which is less than the limitation of the actuator. The simulation duration is set to 200s, and the simulation step size is 0.001s. The trajectories of UAV swarm formation flight are shown in Figure 4. Figure 5 shows the position tracking of all followers. The velocities, flight-path angles, and heading angles of UAV swarm are shown in Figure 6, Figure 7 and Figure 8, respectively.

It can be seen from Figure 4 that all follower UAVs can track the trajectory of the leader UAV by using the finite-time formation control protocol (18). In Figure 5, $x_i - r_{ix}$, $y_i - r_{iy}$, $z_i - z_{ix}$ converge to x_0, y_0, z_0 in finite time, respectively, which means that the desired formation is achieved and maintained. Simulation results show that the velocities, flight-path angles, and heading angles of all follower UAVs can exactly track the items of the leader UAV, where all follower UAVs have lag delay due to input delay. The simulation results verify that the proposed control protocol solves finite-time formation control problem with time-delay.

In order to better show the performance of the proposed finite-time control protocol (18), the following

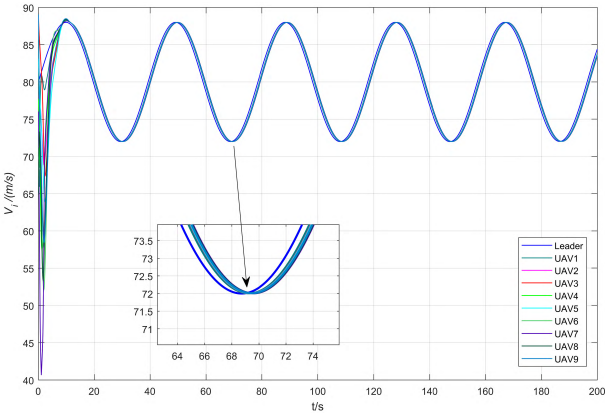

FIGURE 6. The velocities of UAV swarm.

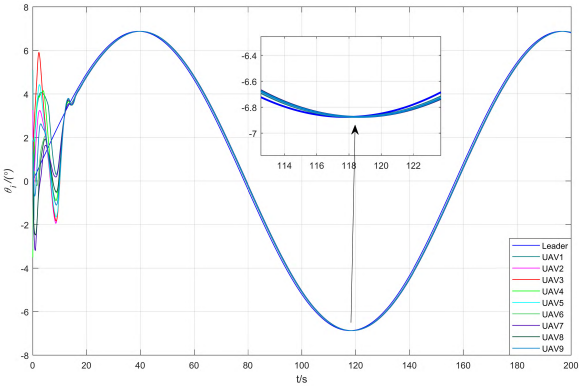

FIGURE 7. The flight-path angles of UAV swarm.

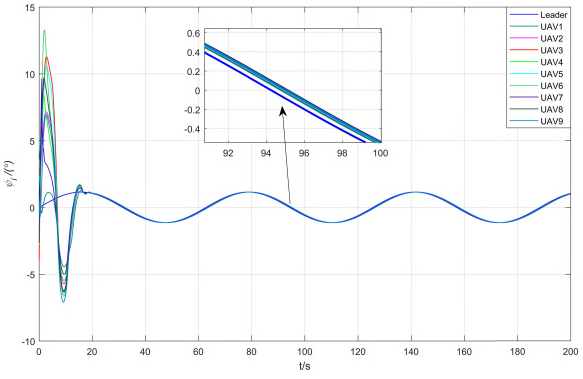

FIGURE 8. The heading angles of UAV swarm.

finite-time formation protocol without saturation constraint is constructed.

$$\begin{pmatrix} u_{ix} \\ u_{iy} \\ u_{iz} \end{pmatrix} = \ddot{\hat{p}}_i - k_1 sig\left(\sum_{j=1}^{N} a_{ij}\left(\left(y_{1i} - y_{1j} - r_{ij}\right) + \tau_i\left(y_{2i} - y_{2j}\right)\right) + a_{i0}\left(y_{1i} - r_i + \tau_i y_{2i}\right)\right)^{\alpha_1} - k_2 sig\left(\sum_{j=1}^{N} a_{ij}\left(y_{2i} - y_{2j}\right) + a_{i0} y_{2i}\right)^{\alpha_2}. \quad (35)$$

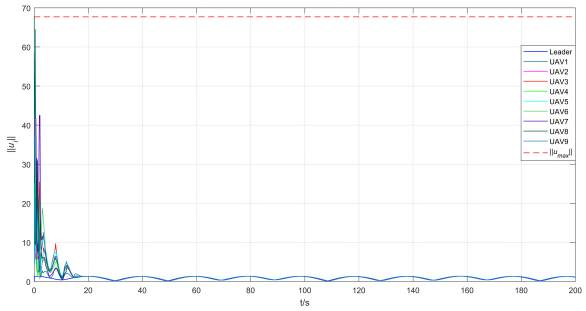

FIGURE 9. The control inputs using control protocol (18).

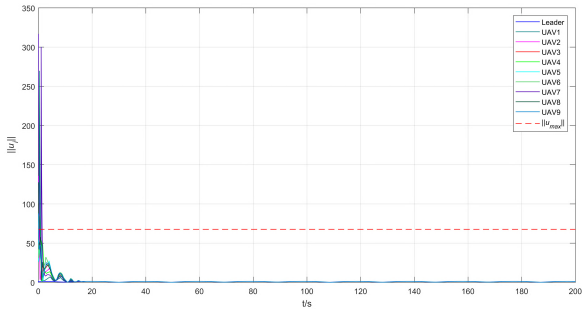

FIGURE 10. The control inputs using control protocol (35).

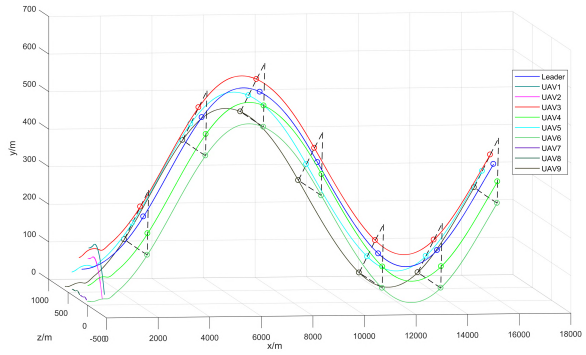

FIGURE 11. The trajectories of UAV swarm formation flight by using (35).

where the design parameters are selected as $k_1 = 5$, $k_2 = 5$, $\alpha_1 = 0.6$, $\alpha_2 = 0.75$. The proof of stability is similar to Theorem 2 and is hence omitted here.

Firstly, we compare the control inputs of control protocols (18) and (35) under the same conditions. The control inputs using control protocol (18) and control protocol (35) are shown in Figure 9, Figure 10, respectively. Figure 9 shows that, using the finite-time control protocol (18), the control input does not exceed the limitation of the actuator. Figure 10 shows that the control input exceeds the limitation of the actuator, which will deteriorate the stability of the controller. The simulation results verify that the proposed protocol can ensure the control input within the limitation of actuator. For a given input saturation, we can satisfy the saturation constraint by choosing parameters.

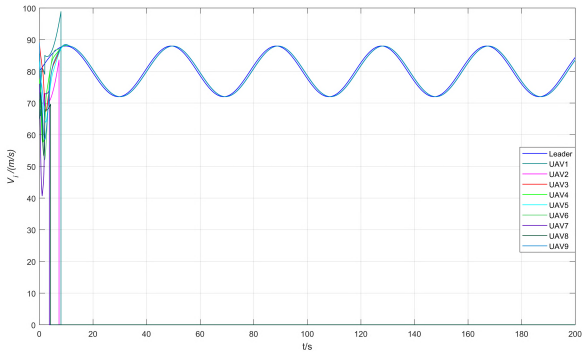

FIGURE 12. The velocities of UAV swarm by using (35).

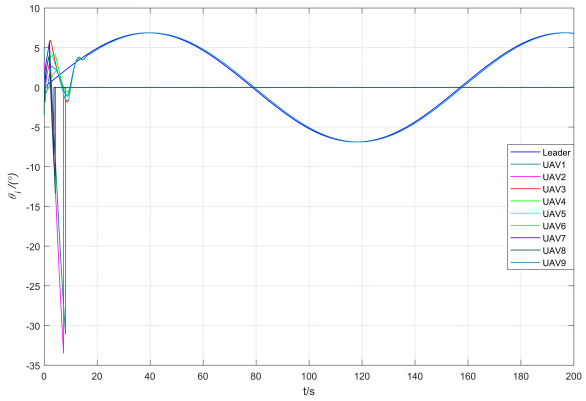

FIGURE 13. The flight-path angles by using (35).

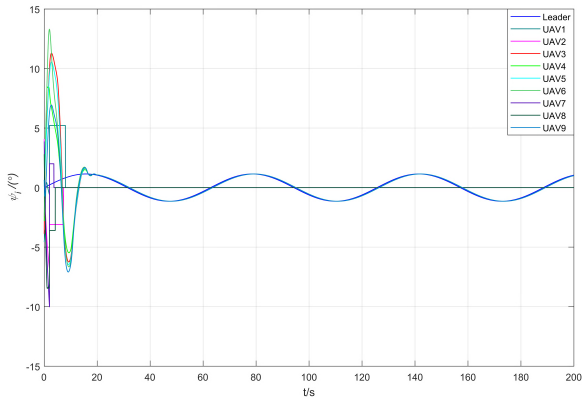

FIGURE 14. The heading angles by using (35).

UAVs are designed with instantaneous maneuver overload in mind, and instantaneous maneuver overload is generally greater than continuous maneuver overload. Assume that the instantaneous limitation of the actuator is $100m/s^2$, and UAV is destroyed when the control input exceeds $100m/s^2$. If the instantaneous input is between $70m/s^2$ and $100m/s^2$, the impact on the actuator of the UAV is considered to be recoverable. The trajectories, velocities, flight-path angles, and heading angles of UAV swarm using (35) are shown in Figure 11, Figure 12, Figure 13, Figure 14, respectively.

From Figure 3, the communication topology is connected after removing the UAVs 1, 2, 7, and 8. It can be seen from Figure 11 that the 1st, 2nd, 7th, and 8th UAVs crash because the control input far exceeded the limitation of the actuator. The remaining 5 UAVs can track the trajectory of the leader UAV. Simulation results of velocities, flight-path angles and heading angles show that the UAVs 1,2,7,8 fly a small distance under the force of gravity and then crash. Comparing the simulation results of the control protocol (18) with the algorithm (35), it can be seen that the proposed control protocol (18) solves finite-time formation control problem with time-delay and input saturation.

V. CONCLUSION

This paper investigated finite-time formation control problems of UAV swarm system with time-delay and input saturation. Linearization model was firstly derived by using precise feedback linearization for the nonlinear model of UAV. Then, fixed-time observer was constructed to estimate the leader UAV's states. By introducing Artstein's transformation, we transformed the delayed second-order system into a delay-free system and then a saturation function was used to tackle the input saturation problem. With Artstein's transformation and saturation function, a novel distributed control protocol was constructed to achieve finite-time formation control. It was proved that the proposed observer and control protocol can achieve finite-time formation control by utilizing homogeneous method and Lyapunov theory. Finally, application into formation control of UAV swarm system was provided to demonstrate the effecttiveness of the proposed method. The problems of finite-time formation control with multiple leaders are future topics to be discussed.

ACKNOWLEDGMENT

The authors would like to thank the reviewers and editors for their valuable comments and suggestions to improve the presentation and theoretical results of this paper.

REFERENCES

[1] L. He, P. Bai, X. Liang, J. Zhang, and W. Wang, "Feedback formation control of UAV swarm with multiple implicit leaders," *Aerosp. Sci. Technol.*, vol. 72, pp. 327–334, Jan. 2018.

[2] F. C. Rossi, A. Fritz, and G. Becker, "Combining satellite and UAV imagery to delineate forest cover and basal area after mixed-severity fires," *Sustainability*, vol. 10, no. 7, p. 2227, Jul. 2018.

[3] M. Saska *et al.*, "System for deployment of groups of unmanned micro aerial vehicles in GPS-denied environments using onboard visual relative localization," *Auton. Robots*, vol. 41, no. 4, pp. 919–944, Apr. 2017.

[4] M. Kabiri, H. Atrianfar, and M. B. Menhaj, "Formation control of VTOL UAV vehicles under switching-directed interaction topologies with disturbance rejection," *Int. J. Control*, vol. 91, no. 1, pp. 33–44, 2018.

[5] S. Park, K. Kim, H. Kim, and H. Kim, "Formation control algorithm of multi-UAV-based network infrastructure," *Appl. Sci.*, vol. 8, no. 10, p. 1740, Oct. 2018.

[6] Y. Wang, L. He, and C. Huang, "Adaptive time-varying formation tracking control of unmanned aerial vehicles with quantized input," *ISA Trans.*, to be published, doi: 10.1016/j.isatra.2018.09.013.

[7] D. Cai, J. Sun, and S. T. Wu, "UAVs formation flight control based on behavior and virtual structure," in *Proc. AsiaSim*, Shanghai, China, 2012, pp. 429–438.

[8] E. Zhao, T. Chao, S. Wang, and M. Yang, "Finite-time formation control for multiple flight vehicles with accurate linearization model," *Aerosp. Sci. Technol.*, vol. 71, pp. 90–98, Dec. 2017.

[9] K. Raghuwaiya, B. Sharma, and J. Vanualailai, "Leader-follower based locally rigid formation control," *J. Adv. Transp.*, vol. 2018, Feb. 2018, Art. no. 5278565, doi: 10.1155/2018/5278565.

[10] A. Askari, M. Mortazavi, and H. A. Talebi, "UAV formation control via the virtual structure approach," *J. Aerosp. Eng.*, vol. 28, no. 1, p. 04014047, Jan. 2015.

[11] Y. Xu and Z. Zhen, "Multivariable adaptive distributed leader-follower flight control for multiple UAVs formation," *Aeronautical J*, vol. 121, no. 1241, pp. 877–900, 2017.

[12] H. Duan and H. Qiu, "Unmanned aerial vehicle distributed formation rotation control inspired by leader-follower reciprocation of migrant birds," *IEEE Access*, vol. 6, pp. 23431–23443, 2018.

[13] J. Hu, X. Sun, and L. He, "Adaptive finite-time control for formation tracking of multiple nonholonomic unmanned aerial vehicles with quantized input signals," *Math. Problems Eng.*, vol. 2018, Jun. 2018, Art. no. 3528092, doi: 10.1155/2018/3528092.

[14] H. Du, W. Zhu, G. Wen, and D. Wu, "Finite-time formation control for a group of quadrotor aircraft," *Aerosp. Sci. Technol.*, vol. 69, pp. 609–616, Oct. 2017.

[15] D. Wang, Q. Zong, B. Tian, S. Shao, X. Zhang, and X. Zhao, "Neural network disturbance observer-based distributed finite-time formation tracking control for multiple unmanned helicopters," *ISA Trans.*, vol. 73, pp. 208–226, Feb. 2018.

[16] M. Fu and L. Yu, "Finite-time extended state observer-based distributed formation control for marine surface vehicles with input saturation and disturbances," *Ocean Eng.*, vol. 159, pp. 219–227, Jul. 2018.

[17] L. Yu and M. Fu, "A robust finite-time output feedback control scheme for marine surface vehicles formation," *IEEE Access*, vol. 6, pp. 41291–41301, 2018.

[18] Y. Huang and Y. Jia, "Distributed finite-time output feedback synchronisation control for six DOF spacecraft formation subject to input saturation," *IET Control Theory Appl.*, vol. 12, no. 4, pp. 532–542, Mar. 2018.

[19] D. Ye, J. Zhang, and Z. Sun, "Extended state observer–based finite-time controller design for coupled spacecraft formation with actuator saturation," *Adv. Mech. Eng.*, vol. 9, no. 4, pp. 1–13, Apr. 2017.

[20] Q. Hu, J. Zhang, and M. I. Friswell, "Finite-time coordinated attitude control for spacecraft formation flying under input saturation," *J. Dyn. Syst., Meas., Control*, vol. 137, no. 6, p. 061012, Jun. 2015.

[21] Y. Su and J. Swevers, "Finite-time tracking control for robot manipulators with actuator saturation," *Robot. Comput.-Integr. Manuf.*, vol. 30, no. 2, pp. 91–98, Apr. 2014.

[22] H. Chen, B. Li, B. Zhang, and L. Zhang, "Global finite-time partial stabilization for a class of nonholonomic mobile robots subject to input saturation," *Int. J. Adv. Robotic Syst.*, vol. 12, p. 159, Nov. 2015.

[23] R. Liu, X. Cao, and M. Liu, "Finite-time synchronization control of spacecraft formation with network-induced communication delay," *IEEE Access*, vol. 5, pp. 27242–27253, 2017.

[24] J. Zhang, D. Ye, M. Liu, and Z. Sun, "Adaptive fuzzy finite-time control for spacecraft formation with communication delays and changing topologies," *J. Franklin Inst.*, vol. 354, no. 11, pp. 4377–4403, Jul. 2017.

[25] J. Wang, J. Fu, and G. Zhang, "Finite time consensus problem for multiple non-holonomic agents with communication delay," *J. Syst. Sci. Complex.*, vol. 28, no. 3, pp. 559–569, Jun. 2015.

[26] S. Li, H. Du, and X. Lin, "Finite-time consensus algorithm for multi-agent systems with double-integrator dynamics," *Automatica*, vol. 47, no. 8, pp. 1706–1712, Aug. 2011.

[27] Y. Hong, Y. Xu, and J. Huang, "Finite-time control for robot manipulators," *Syst. Control Lett.*, vol. 46, no. 4, pp. 243–253, Jul. 2002.

[28] Z. Zuo and L. Tie, "Distributed robust finite-time nonlinear consensus protocols for multi-agent systems," *Int. J. Syst. Sci.*, vol. 47, no. 6, pp. 1366–1375, Apr. 2016.

[29] X. Wang, J. Li, J. Xing, and R. Wang, "A novel finite-time average consensus protocol based on event-triggered nonlinear control strategy for multiagent systems," *J. Inequal. Appl.*, vol. 2017, no. 1, p. 258, Dec. 2017. [Online]. Available: https://link.springer.com/journal/13660/2017/1/page/3

[30] Y. Cheng, R. Jia, H. Du, G. Wen, and W. Zhu, "Robust finite-time consensus formation control for multiple nonholonomic wheeled mobile robots via output feedback," *Int. J. Robust Nonlinear Control*, vol. 28, no. 6, pp. 2082–2096, 2018.

[31] E. Moulay, M. Dambrine, N. Yeganefar, and W. Perruquetti, "Finite-time stability and stabilization of time-delay systems," *Syst. Control Lett.*, vol. 57, no. 7, pp. 561–566, 2008.
[32] J. Ni, L. Liu, C. Liu, and J. Liu, "Fixed-time leader-following consensus for second-order multiagent systems with input delay," *IEEE Trans. Ind. Electron.*, vol. 64, no. 11, pp. 8635–8646, Nov. 2017.
[33] B. Arévalo, P. J. Cruz, and P. Leica, "Sliding mode formation control of mobile robots with input delays," in *Proc. ETCM*, Salinas, Ecuador, Oct. 2017, pp. 1–6.
[34] R. Xue, J. Song, and G. Cai, "Distributed formation flight control of multi-UAV system with nonuniform time-delays and jointly connected topologies," *Proc. Inst. Mech. Eng., G, J. Aerosp. Eng.*, vol. 230, no. 10, pp. 1871–1881, Aug. 2015.
[35] Q. Zhou, H. Li, C. Wu, L. Wang, and C. K. Ahn, "Adaptive fuzzy control of nonlinear systems with unmodeled dynamics and input saturation using small-gain approach," *IEEE Trans. Syst., Man, Cybern., Syst.*, vol. 47, no. 8, pp. 1979–1989, Aug. 2017.
[36] A. Sharghi, M. Baradarannia, and F. Hashemzadeh, "Leader-follower fixed-time consensus for multi-agent systems with heterogeneous nonlinear inherent dynamics," in *Proc. ISCMI*, Dubai, United Arab Emirates, Nov. 2016, pp. 224–228.
[37] Y. Shang, "Fixed-time group consensus for multi-agent systems with nonlinear dynamics and uncertainties," *IET Control Theory Appl.*, vol. 12, no. 3, pp. 395–404, 2018.
[38] V. Lechappé, E. Moulay, F. Plestan, A. Glumineau, and A. Chriette, "New predictive scheme for the control of LTI systems with input delay and unknown disturbances," *Automatica*, vol. 52, pp. 179–184, Feb. 2015.
[39] Z. Artstein, "Linear systems with delayed controls: A reduction," *IEEE Trans. Autom. Control*, vol. 27, no. 4, pp. 869–879, Aug. 1982.
[40] E. Cruz-Zavala, J. A. Moreno, and L. M. Fridman, "Uniform robust exact differentiator," *IEEE Trans. Autom. Control*, vol. 56, no. 11, pp. 2727–2733, Nov. 2011.
[41] G. E. Forsythe, M. A. Malcolm, and C. B. Moler, "Numerical integration," in *Computer Methods for Mathematical Computations*, Englewood Cliffs, NJ, USA: Prentice-Hall, 1977, ch. 5, sec. 1, pp. 85–89.
[42] L. Rosier, "Homogeneous Lyapunov function for homogeneous continuous vector field," *Syst. Control Lett.*, vol. 19, no. 6, pp. 467–473, 1992.
[43] S. Bhat and D. S. Bernstein, "Finite-time stability of homogeneous systems," in *Proc. Amer. Control Conf.*, Albuquerque, NM, USA, Jun. 1997, pp. 2513–2514.
[44] S. P. Bhat and D. S. Bernstein, "Finite-time stability of continuous autonomous systems," *SIAM J. Control Optim.*, vol. 38, no. 3, pp. 751–766, Jan. 2000.
[45] H. Ha, J. S. Welsh, and M. Alamir, "Useful redundancy in parameter and time delay estimation for continuous-time models," *Automatica*, vol. 95, pp. 455–462, Sep. 2018.
[46] L. Belkoura, J.-P. Richard, and M. Fliess, "Parameters estimation of systems with delayed and structured entries," *Automatica*, vol. 45, no. 5, pp. 1117–1125, May 2009.
[47] Z. Zuo, C. Wang, and Z. Ding, "Robust consensus control of uncertain multi-agent systems with input delay: A model reduction method," *Int. J. Robust Nonlinear Control*, vol. 27, no. 11, pp. 1874–1894, Jul. 2017.

AN ZHANG was born in Baoji, China, in 1962. He received the M.S. degree in systems engineering and the Ph.D. degree in control theory and control engineering from Northwestern Polytechnical University, Xi'an, China, in 1986 and 1999, respectively. He is currently a full-time Professor of control engineering with Northwestern Polytechnical University. He has authored or co-authored 31 refereed papers in journals and in international conference proceedings. His current research interests include multiagent systems, nonlinear control systems, intelligent control, and UAV control.

DING ZHOU was born in Kaifeng, China, in 1991. He received the B.S. and M.S. degrees in control engineering from Northwestern Polytechnical University, Xi'an, China, in 2017, where he is currently pursuing the Ph.D. degree in control theory. His current research interests include multiagent systems and the formation control of UAV.

MI YANG was born in Tongchuan, China, in 1995. She received the B.S. degree in safety engineering from Northwestern Polytechnical University, Xi'an, China, in 2017, where she is currently pursuing the Ph.D. degree in control theory. Her current research interests include formation control and multiagent systems.

PAN YANG was born in Xianyang, China, in 1996. She received the B.S. degree in electrical engineering and automation from Northwestern Polytechnical University, Xi'an, China, in 2017, where she is currently pursuing the Ph.D. degree in control theory. Her current research interests include UAV swarm and coverage control.